SPANDIDOS PUBLICATIONS

INTERNATIONAL JOURNAL OF ONCOLOGY 51: 1146-1158, 2017

Disrupting mitochondrial Ca^{2+} homeostasis causes tumor-selective TRAIL sensitization through mitochondrial network abnormalities

YOHEI OHSHIMA[1], NATSUHIKO TAKATA[1], MIKI SUZUKI-KARASAKI[1,2], YUKIHIRO YOSHIDA[1], YASUAKI TOKUHASHI[1] and YOSHIHIRO SUZUKI-KARASAKI[2,3]

[1]Department of Orthopedic Surgery, Nihon University School of Medicine, Tokyo 173-8610; [2]Plasma ChemiBio Laboratory, Nasushiobara, Tochigi 329-2813; [3]Division of Physiology, Department of Biomedical Sciences, Nihon University School of Medicine, Tokyo 173-8610, Japan

Received March 7, 2017; Accepted July 24, 2017

DOI: 10.3892/ijo.2017.4096

Abstract. The tumor necrosis factor-related apoptosis-inducing ligand (TRAIL) has emerged as a promising anticancer agent with high tumor-selective cytotoxicity. The congenital and acquired resistance of some cancer types including malignant melanoma and osteosarcoma impede the current TRAIL therapy of these cancers. Since fine tuning of the intracellular Ca^{2+} level is essential for cell function and survival, Ca^{2+} dynamics could be a promising target for cancer treatment. Recently, we demonstrated that mitochondrial Ca^{2+} removal increased TRAIL efficacy toward malignant melanoma and osteosarcoma cells. Here we report that mitochondrial Ca^{2+} overload leads to tumor-selective sensitization to TRAIL cytotoxicity. Treatment with the mitochondrial Na^{+}/Ca^{2+} exchanger inhibitor CGP-37157 and oxidative phosphorylation inhibitor antimycin A and FCCP resulted in a rapid and persistent mitochondrial Ca^{2+} rise. These agents also increased TRAIL sensitivity in a tumor-selective manner with a switching from apoptosis to a nonapoptotic cell death. Moreover, we found that mitochondrial Ca^{2+} overload led to increased mitochondrial fragmentation, while mitochondrial Ca^{2+} removal resulted in mitochondrial hyperfusion. Regardless of their reciprocal actions on the mitochondrial dynamics, both interventions commonly exacerbated TRAIL-induced mitochondrial network abnormalities. These results expand our previous study and suggest that an appropriate level of mitochondrial Ca^{2+} is essential for maintaining the mitochondrial dynamics and the survival of these cells. Thus, disturbing mitochondrial Ca^{2+} homeostasis may serve as a promising approach to overcome the TRAIL resistance of these cancers with minimally compromising the tumor-selectivity.

Correspondence to: Dr Yoshihiro Suzuki-Karasaki, Plasma ChemiBio Laboratory, 398 Takaatsu, Nasushiobara, Tochigi 329-2813, Japan
E-mail: suzuki-yoshihiro@opal.plala.or.jp; suzuki.yoshihiro@nihon-u.ac.jp

Key words: TRAIL, mitochondria, Ca^{2+}, mitochondrial dynamics, tumor-selective killing

Introduction

The tumor necrosis factor-related apoptosis-inducing ligand (TRAIL) is a cytokine that belongs to the tumor necrosis factor superfamily. TRAIL has emerged as a promising cancer-selective anticancer drug. It inhibits cell proliferation and induces cell death in a variety of cancer cell types while has minimal cytotoxicity toward normal cells (1-4). TRAIL primarily triggers the extrinsic and intrinsic apoptotic pathways by binding to two death receptors (DRs), TRAIL receptor (TRAIL-R)1/DR4 and TRAIL-R2/DR5 (5,6). TRAIL has also been shown to trigger other cell death modalities including autophagy (7,8) and necroptosis (9,10) in some cancers. Different cancers including malignant melanoma (MM) and osteosarcoma (OS) cells are resistant to TRAIL-induced apoptosis (11-15). Accordingly, the combined use of a certain drug that enables to alleviate drug resistance is essential for effective TRAIL therapy of these cancers.

Ca^{2+} is an essential intracellular second messenger whose level is tightly regulated. Finely and spatiotemporally tuning of Ca^{2+} results in short and synchronized Ca^{2+} waves, which are primarily required for energy production, cell function and survival (16). On the other hand, a significant and persistent increase in Ca^{2+} is a master cause of cell death. An excessive rise in mitochondrial Ca^{2+} concentration ($[Ca^{2+}]_{mit}$) results in increased permeability of the inner mitochondrial membrane. The mitochondrial permeability transition (MPT) in turn leads to a rapid collapse of mitochondrial membrane potential, loss of ATP, osmotic rupture of the outer mitochondrial membrane. Ultimately, the loss of ATP and the fall of the mitochondrial integrity lead to necrosis (17,18). Mitochondrial Ca^{2+} overload also causes apoptosis. The rupture of the outer mitochondrial membrane can result in the release of different pro-apoptotic proteins such as cytochrome *c* and apoptosis-inducing factor (19). Recent evidence suggests that Ca^{2+} also plays a regulatory role in other cell death modalities such as autophagy and anoikis (20). Moreover, different cancer cell

types exhibit tumor-specific traits in Ca^{2+} dynamics, which contribute to tumorigenesis, malignant phenotypes, drug resistance, increased proliferation, evasion from apoptosis and survival (21). Thus, Ca^{2+} is emerging as a new target for cancer treatment (22,23). Ca^{2+} dynamics in MM and OS and the role of Ca^{2+} in TRAIL cytotoxicity toward these two cancers remain largely unclear. Previously, we showed that acute TRAIL treatment increased both $[Ca^{2+}]_{cyt}$ and $[Ca^{2+}]_{mit}$ in several human MM and OS cell lines (24). Unexpectedly, the Ca^{2+} signals served as a pro-survival factor rather than a pro-apoptotic factor, since overall Ca^{2+} removal or specific removal of mitochondrial Ca^{2+} sensitized these cells to TRAIL cytotoxicity. Our data suggested that the two cancer cell types were resistant to mitochondrial Ca^{2+} overload caused by TRAIL.

Mitochondria are dynamic organelles whose structure is regulated by a mechanic mechanism encompassing fission and fusion processes. Mitochondrial network homeostasis is critical for cell function and survival (25) since it is essential for maintaining mitochondrial functions such as energy supply and metabolic activity. Mitochondrial dynamics is regulated by dynamin-related proteins with GTPase activity. Dynamin-related protein 1 (Drp1) regulates mitochondrial fission, while mitofusin 1/2 and optic atrophy 1 control mitochondrial fusion and cristae organization (26). It is widely accepted that cancer cells alter mitochondrial dynamics to resist apoptosis and adapt their nonphysiological bioenergetics microenvironments (27). Accordingly, disruption of the mitochondrial dynamics may be a promising strategy to target apoptosis-resistant cancer cells. Indeed, increasing body of evidence indicates that inhibiting mitochondrial fission and fusion regulators cause a severe mitochondrial dysfunction and apoptosis in a variety of cancer cell types. However, the role of mitochondrial fission in apoptosis is a matter of debate. Mitochondrial fission exhibits inverse (pro-apoptotic or anti-apoptotic) functions depending on the cell type and the applied apoptotic stimuli (28-32). Previously, we demonstrated that TRAIL evokes mitochondrial fragmentation in a tumor-selective manner and that inhibition or knockdown of Drp1 caused mitochondrial hyperfusion and sensitized MM and OS cells to TRAIL-induced apoptosis (33,34). These observations suggest that mitochondrial fission is a critical pro-survival event in these cancer cells upon TRAIL treatment. In this study, we investigated the mechanisms of the resistance to mitochondrial Ca^{2+} overload with a particular interest in the relevance to mitochondrial dynamics. Here we report that mitochondrial Na^{+}/Ca^{2+} exchanger (NCLX) plays a pivotal role in the resistance to mitochondrial Ca^{2+} overload. Eventually, blockade of NCLX caused mitochondrial Ca^{2+} overload and sensitized MM and OS cells to TRAIL cytotoxicity. Moreover, we found that mitochondrial Ca^{2+} overload and removal regulated mitochondrial fission positively and negatively, respectively while commonly exacerbated TRAIL-induced mitochondrial network abnormalities, apoptosis, and non-apoptotic cell death.

Materials and methods

Materials. Soluble recombinant human TRAIL was obtained from Enzo Life Sciences (San Diego, CA, USA). Agonistic anti-human TRAIL-R2/TNFRSF10B antibody (clone 71903 #MAB631-100) was purchased from R&D Systems (Minneapolis, MN, USA). Antimycin A, FCCP, and the pan-caspase-inhibitor z-VAD-fluoromethylketone (Z-VAD-FMK) were obtained from Sigma-Aldrich (St. Louis, MO, USA). All insoluble reagents were dissolved in dimethylsulfoxide and diluted with high glucose-containing Dulbecco's modified Eagle's medium (Sigma-Aldrich) supplemented with 10% fetal bovine serum (Sigma-Aldrich; FBS/DMEM) or Hank's balanced salt solution (HBSS) (pH 7.4) to a final concentration of <0.1% before use.

Cell culture. Human MM (A375, A2058, SK-MEL-2) and OS (MG63, SAOS-2, HOS) cell lines and WI-38 fibroblasts were obtained from Health Science Research Resource Bank (Osaka, Japan). Human TE85 and 143B OS cells were kindly gifted by Dr T. Ando (Yamanashi University). Human dermal fibroblasts (HDF) from facial dermis were obtained from Cell Applications (San Diego, CA, USA). These cells were cultured in FBS/DMEM supplemented with 100 U/ml penicillin and 100 μg streptomycin (Thermo Fisher Scientific, Rochester, NY, USA) in a 5% CO_2 incubator. Cells were harvested by incubating with 0.25% trypsin-EDTA (Thermo Fisher Scientific) for 5 min at 37˚C.

Ca^{2+} measurements. Changes in $[Ca^{2+}]_{cyt}$ and $[Ca^{2+}]_{mit}$ levels were measured using Fluo 4-AM and rhod 2-AM (Dojindo Kumamoto, Japan), respectively as previously described (24). For improvement of mitochondrial localization of rhod 2-AM, it was reduced to the colorless, nonfluorescent dihydrorhod 2-AM by sodium borohydride, according to the manufacturer's protocol. Cells were loaded with 4 μM each of Fluo 4-AM or dihydrorhod 2-AM for 40 min at 37˚C, washed with HBSS. Then, the cells ($1x10^6$/ml) were resuspended in HBSS in 96-well plates. The cells were manually added with the agents to be tested. Then, the cells were measured for fluorescence in a microplate reader (Fluoroskan Ascent, Thermo Fisher Scientific) with excitation and emission at 485 and 538 nm (for Fluo 4-AM) and 542 and 592 nm (for rhod 2-AM), respectively.

Cell viability and apoptosis measurements. Cell growth was measured by WST-8 assay using Cell Counting Reagent SF (Nacalai Tesque, Kyoto, Japan) as previously described (24). This method is a colorimetric assay based on the formation of a water-soluble formazan product. Briefly, cells ($8x10^3$/well) were seeded in 96-well plates and cultured with the agents to be tested for 72 h at 37˚C in a 5% CO_2 incubator. Then 1/10 volume of WST-8 reagent was added, incubated for 1 h at 37˚C and absorbance at 450 nm was measured using a microplate reader (ARVO MX, Perkin-Elmer Japan).

Caspase-3/7 activation, membrane integrity, and cell death assay. Caspase-3/7 activation, membrane integrity, and cell death were simultaneously measured by Muse™ Cell Analyzer (Merck Millipore, Darmstadt, Germany) using Muse Caspase-3/7 kit as previously described (24). Briefly, cells ($1x10^5$/ml) in 24-well plates were treated with the agents to be tested for 24 h in 10% FBS/DMEM at 37˚C and then stained with a novel caspase-3/7 reagent NucView™ and 7-amino-actinomycin D (7-AAD), a dead cell marker in the kit. 7-AAD is excluded from healthy and early apoptotic cells,

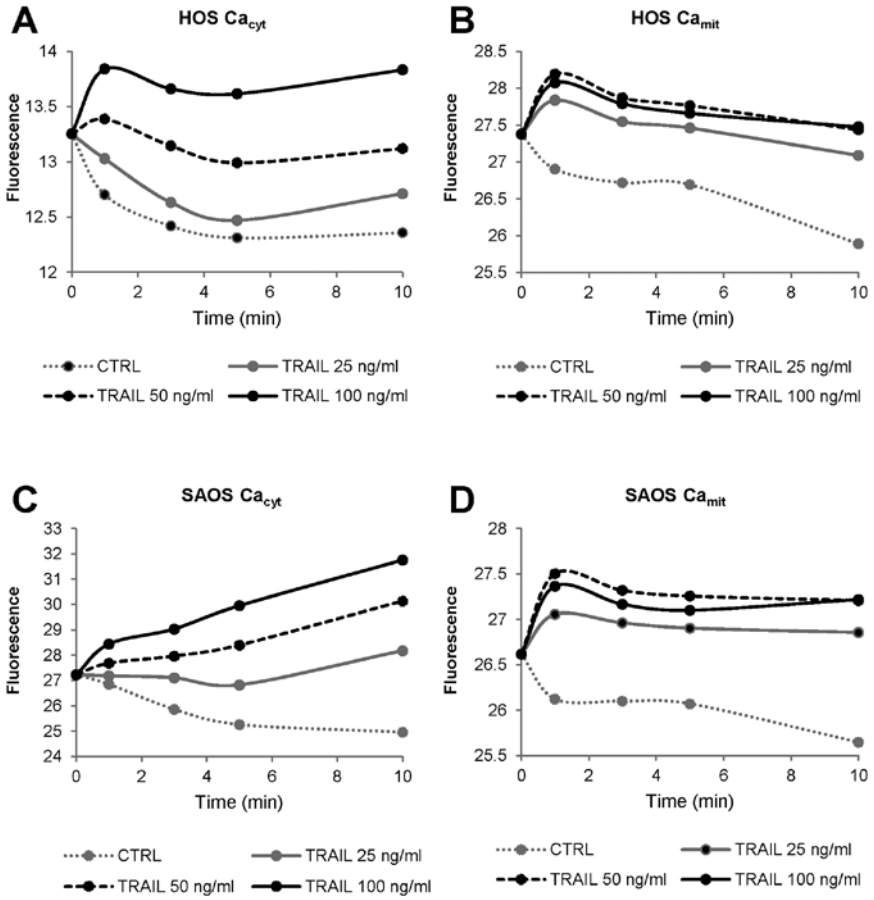

Figure 1. TRAIL-resistant malignant cells are tolerant to mitochondrial Ca^{2+} overload. HOS (A and B) and SAOS-2 cells (C and D) were loaded with 4 μM Fluo 4-AM (A and C) and dihydrorhod 2-AM (B and D), respectively for 40 min at 37˚C, washed with HBSS. The dye-loaded cells (1x10^6/ml) were resuspended in the Ca^{2+}-containing medium in 96-well plates. The cells were added to 25, 50 or 100 ng/ml TRAIL and immediately measured for fluorescence in triplicate in a microplate reader at 0, 1, 2, 3, 5 and 10 min with excitation and emission at 485 and 538 nm, respectively (for Fluo 4-AM) and 542 and 592 nm, respectively (for dihydrorhod 2-AM). The data are representative of 3 independent experiments with similar results.

while permeates late apoptotic and dead cells. Accordingly, four cell populations can be distinguished by the kit; live cells, caspase$^-$/7-AAD$^-$; early apoptotic cells, caspase$^+$/7-AAD$^-$; late apoptotic/dead cells, caspase$^+$/7-AAD$^+$; necrotic cells, caspase$^-$/7-AAD$^+$.

Live-cell mitochondrial network imaging. The mitochondrial network was analyzed as previously described (34) with minor modifications. Briefly, cells in FBS/DMEM (3x10^4/well) adherent on 8-well chambered coverslips were treated with the agents to be tested for 24 h at 37˚C in a 5% CO_2 incubator. After removing the medium by aspiration, the cells were washed with fresh FBS/DMEM and stained with 20 nM MitoTracker Red CMXRos for 1 h at 37˚C in the dark in a 5% CO_2 incubator. The cells were then washed with and immersed in FluoroBrite™ DMEM (Thermo Fisher Scientific). Images were obtained using a BZ X-700 Fluorescence Microscope (Keyence, Osaka, Japan) equipped with a 100x, 1.40 n.a. UPlanSApo Super-Apochromat, coverslip-corrected oil objective (Olympus, Tokyo, Japan). Images were analyzed using BZ-H3A application software (Keyence) and free NIH ImageJ software (NIH, Bethesda, MD, USA).

Statistical analysis. Data were analyzed by one-way analysis of variance followed by the Tukey's post hoc test using an add-in software for Excel 2016 for Windows (SSRI, Tokyo, Japan). All values were expressed as means ± SD and $P<0.05$ was considered to be significant.

Results

TRAIL-resistant tumor cells are highly tolerant to mitochondrial Ca^{2+} overload by the drug. Previously, we demonstrated that TRAIL induces $[Ca^{2+}]_{cyt}$ and $[Ca^{2+}]_{mit}$ in several MM and OS cell lines in a dose-dependent manner (24). However, we noticed that in different cell lines the effects of TRAIL on $[Ca^{2+}]_{cyt}$ and $[Ca^{2+}]_{mit}$ were not always in parallel. Therefore, we studied the impact of TRAIL on $[Ca^{2+}]_{cyt}$ and $[Ca^{2+}]_{mit}$ in more detail. The cells were loaded with Ca^{2+} probes, added with the agents to be tested, and analyzed for their fluorescence in a microplate fluorescence reader. This manual addition alone led to an immediate and transient increase in $[Ca^{2+}]_{cyt}$, probably owing to a mechanical stress-sensitive cation channel. After that, $[Ca^{2+}]_{cyt}$ returned to the baseline within 3-5 min. On the other hand, $[Ca^{2+}]_{cyt}$ was minimally changed for at least the initial 10 min when the cells were allowed to stand without any addition of the materials. Throughout this study, we monitored early Ca^{2+} responses including this tentative mechanical $[Ca^{2+}]_{cyt}$ changes. Fig. 1 shows representative results in HOS and SAOS-2 cells. TRAIL increased $[Ca^{2+}]_{cyt}$ in a dose-depen-

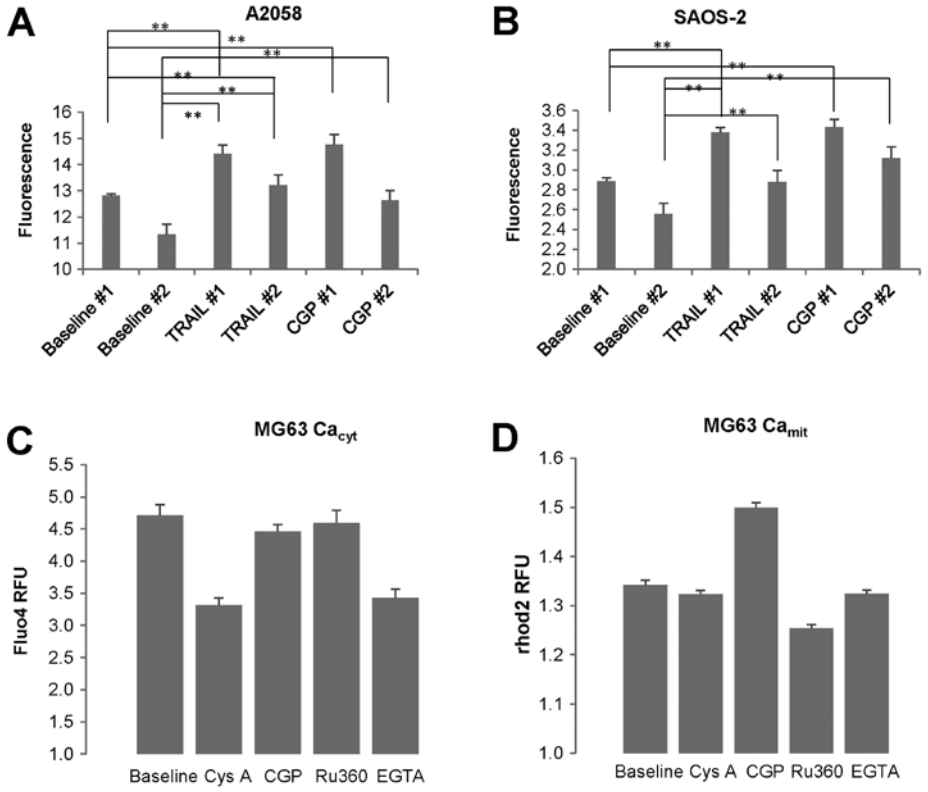

Figure 2. CGP-37157 preferentially increases $[Ca^{2+}]_{mit}$. (A and B) Dihydrorhod 2-AM-loaded A2058 (A) and SAOS-2 (B) cells were resuspended in the Ca^{2+}-containing medium in 96-well plates. The cells were added to 100 ng/ml TRAIL or 10 μM CGP-37157 (CGP) and measured for fluorescence in triplicate. The data represent means ± SD of the calculated fluorescence for 10^6 cells in a representative experiment (N=3). Data were analyzed by ANOVA followed by the Tukey's post hoc test. $^{**}P<0.01$ vs. baseline. (C and D) MG63 cells were loaded with Fluo 4-AM (C) or dihydrorhod 2-AM (D) and resuspended in the Ca^{2+}-containing medium. The cells were added to 1 μM cyclosporine A (CysA), 1 μM Ruthenium 360 (Ru360), 10 μM CGP-37157 (CGP) or 0.5 mM EGTA (C and D), and measured for fluorescence in triplicate. The data represent means ± SD of the average fluorescence value for 3 min in a representative experiment (N=3).

dent manner with the minimal effective dose of 25 ng/ml (Fig. 1A and C), while it increased $[Ca^{2+}]_{mit}$ maximally at 50 ng/ml (Fig. 1B and D). Strikingly, under the conditions, the basal $[Ca^{2+}]_{mit}$ in control cells declined gradually over time. Whereas, relatively TRAIL-sensitive cells including A375 cells, the basal $[Ca^{2+}]_{mit}$ was unchanged at least for 10 min, and $[Ca^{2+}]_{mit}$ elevated in parallel with $[Ca^{2+}]_{cyt}$ in response to TRAIL (data not shown). Collectively, these findings suggest that TRAIL-resistant tumor cells are highly tolerant to mitochondrial Ca^{2+} overload.

CGP-37157 causes mitochondrial Ca^{2+} overload in MM and OS cells. NCLX plays a fundamental role in Ca^{2+} extrusion from the mitochondria in a variety of cell types (35-37). Also, we previously observed that treatment with CGP-37157, a specific inhibitor of NCLX, led to a substantial increase in $[Ca^{2+}]_{mit}$ in OS cells (24). Therefore, we hypothesized that increased Ca^{2+} efflux through NCLX might contribute to the tolerance of mitochondrial Ca^{2+} overload in TRAIL-resistant cells. As mentioned above, in some experiments (Exp #1) the basal $[Ca^{2+}]_{mit}$ in SAOS-2 cells was kept throughout the time monitored (10 min), while in other tests (Exp #2) it was declined over time. In any case, $[Ca^{2+}]_{mit}$ became significantly higher in response to CGP-37157 compared with the corresponding baseline (Fig. 2A and B). We obtained similar results in A2058 and all OS cell lines tested. CGP-37157 treatment increased $[Ca^{2+}]_{mit}$ but not $[Ca^{2+}]_{cyt}$ (Fig. 2C and D). On the other hand, ruthenium 360 (Ru360) decreased $[Ca^{2+}]_{mit}$, but not $[Ca^{2+}]_{cyt}$, while EGTA and cyclosporine A (CysA) reduced both $[Ca^{2+}]_{cyt}$ and $[Ca^{2+}]_{mit}$. These results indicate that Ca^{2+} extrusion through NCLX plays a pivotal role in regulating $[Ca^{2+}]_{mit}$ in MM and OS cells.

CGP-37157 enhances TRAIL cytotoxicity in a tumor-selective manner. Next, we examined the effect of CGP-37157 on TRAIL cytotoxicity. WST-8 assay revealed that treatment with TRAIL 25 and 100 ng/ml for 72 h led to a robust decrease in the viability of SK-MEL-2 cells (50 and 70% reduction, respectively) (Fig. 3A). The three OS cell lines tested (HOS, TE85, 143B) were highly resistant to TRAIL cytotoxicity while SAOS-2 cells were moderately resistant. At 100 ng/ml TRAIL decreased the viability of SAOS-2 cells moderately (maximum of 40% reduction) (Fig. 3B). Whereas, the TRAIL treatment led to only a modest decline (<15%) in their viability or rather increased growth in TE85 and 143B cells (Fig. 3C and D). CGP-37157 treatment ≤10 μM alone for 72 h minimally affected cell growth. However, this compound significantly amplified TRAIL cytotoxicity regardless of cancer cell types (Fig. 3A-D). We observed a smaller amplification of TRAIL-induced cell death in moderately TRAIL-sensitive MM and OS cell lines such as A375 and SAOS-2 cells during the initial 24 h, and the pan-caspase-inhibitor Z-VAD-FMK abrogated the effect completely (Fig. 3E and F). Moreover, flow cytometric analyses

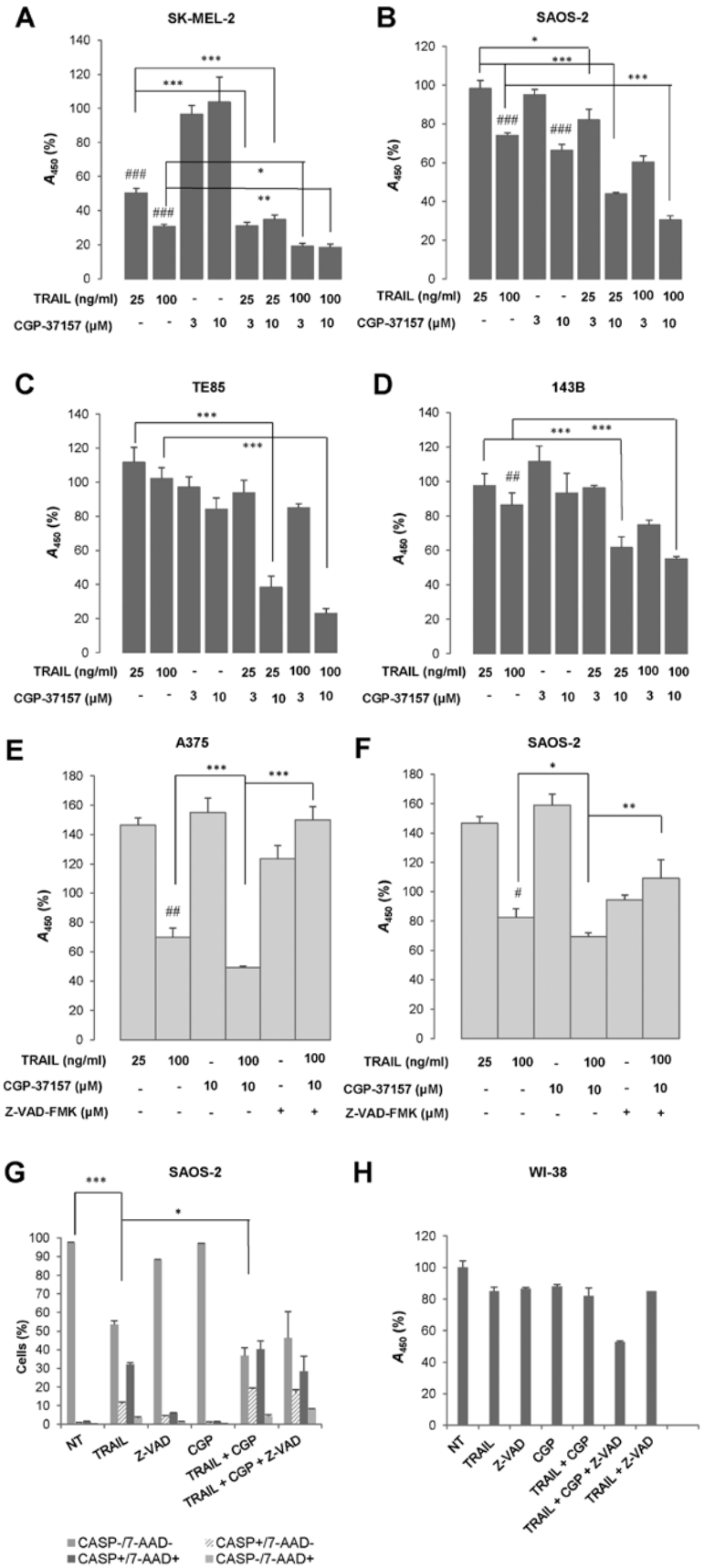

Figure 3. CGP-37157 enhances TRAIL cytotoxicity in a tumor-selective manner. SK-MEL-2 (A), SAOS-2 (B and F), TE85 (C), 143B (D), and A375 cells (E) were treated with 25 and 100 ng/ml TRAIL, 3 and 10 μM CGP-37157 alone or in combination in the presence or absence of 10 μM z-VAD-FMK for 72 h. Then, the cells were analyzed for viability using WST-8 assay in triplicates. The data show means ± SD in a representative experiment (N=3). Data were analyzed by ANOVA followed by the Tukey's post hoc test. *P<0.05; **P<0.01; ***P<0.001; $^{\#\#}$P<0.01; $^{\#\#\#}$P<0.001 vs. non-treated control. (G and H) SAOS-2 cells (G) and WI-38 (H) were treated with 100 ng/ml TRAIL and 10 μM CGP-37157 (CGP) alone or in combination in the presence or absence of 10 μM z-VAD-FMK (Z-VAD) for 72 h. Then the cells were analyzed for caspase-3/7 activation and membrane integrity using NucView and 7-amino-actinomycin D (7-AAD) in a Muse Cell Analyzer (G) and measured for viability using WST-8 assay (H), respectively in triplicates. The data show means ± SD in a representative experiment (N=3). Data were analyzed by ANOVA followed by the Tukey's post hoc *P<0.05; ***P<0.001.

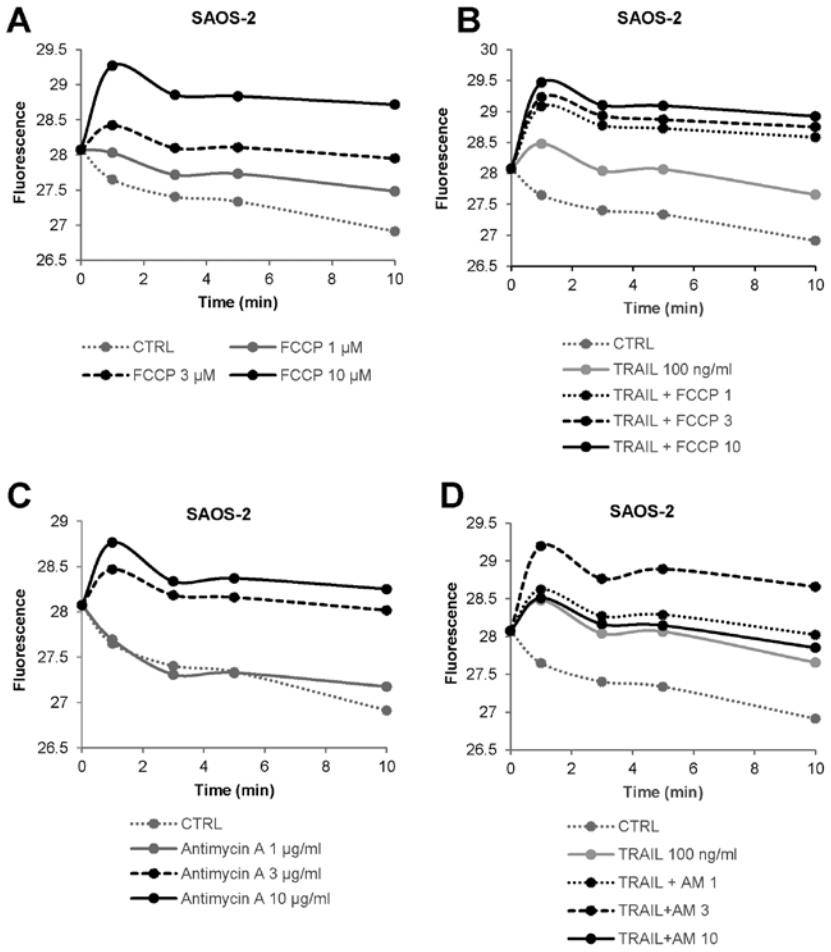

Figure 4. OXOPHOS inhibitors increase and cooperatively modulate $[Ca^{2+}]_{mit}$. Dihydrorhod 2-AM-loaded SAOS-2 cells were treated with 100 ng/ml TRAIL and 1, 3 and 10 μM FCCP (A and B) or 1, 3 and 10 μg/ml antimycin A (AM) (C and D) alone or in combination and measured for fluorescence in triplicate. The data are representative of 3 independent experiments with similar results.

using a caspase-3/7-specific substrate showed that CGP-37157 significantly amplified TRAIL-induced caspase-3/7 activation (Fig. 3G). This effect became pronounced over time. Simultaneous measurement using 7-AAD, a cell membrane damage/death marker, revealed that the cell populations corresponding to both early and late apoptotic cells were increased, but the increases were blocked by Z-VAD-FMK only partially. In contrast to MM and OS cells, TRAIL and CGP-37157 alone or in combination had the minimal effects on the growth of WI-38 fibroblasts (Fig. 3H). These results show that CGP-37157 enhances TRAIL cytotoxicity in a tumor-selective manner.

OXOPHOS inhibitors increase and cooperatively modulate $[Ca^{2+}]_{mit}$ in MM and OS cells. Classic OXOPHOS inhibitors such as antimycin A, CCCP, and FCCP sensitize different tumor cell types including MM and OS cells to TRAIL cytotoxicity (38-40). These facts led us to investigate the possible impact of OXOPHOS inhibitors on mitochondrial Ca^{2+} dynamics. FCCP at concentrations ranging from 1 to 10 μM resulted in a rapid and persistent increase in $[Ca^{2+}]_{mit}$ in SAOS-2 cells in a dose-dependent manner (Fig. 4A). The effect of 3 μM FCCP was almost comparable to that of 100 ng/ml TRAIL (Fig. 4B). The combined use of TRAIL and FCCP led to a greater extent of $[Ca^{2+}]_{mit}$ rise except for 10 μM FCCP compared with either agent alone. Antimycin A also increased $[Ca^{2+}]_{mit}$ in a dose-dependent manner (Fig. 4C). The agent at 3 μg/ml was equivalently potent to 100 ng/ml TRAIL (Fig. 4D). Also, TRAIL + antimycin A was more efficient than either agent alone in increasing $[Ca^{2+}]_{mit}$ except for 10 μg/ml of antimycin A, at which the combined use had a lesser effect than antimycin A alone. We obtained similar results in A2058 and several OS cell lines (data not shown). These results indicate that OXOPHOS inhibitors increase and cooperatively modulate $[Ca^{2+}]_{mit}$ in MM and OS cells.

OXOPHOS inhibitors potentiate TRAIL cytotoxicity in a tumor-selective manner. Then, we examined whether the OXOPHOS inhibitors affected TRAIL cytotoxicity toward MM and OS cells. Treatment with antimycin A (≥1 μg/ml) for 72 h decreased the viability of A375 cells in a dose-dependent manner while FCCP (≥3 μM) reduced it moderately (57%) (Fig. 5A). Moreover, the combined application of TRAIL and either agent except for FCCP (1 μM) decreased the viability almost entirely (>90% reduction). Highly TRAIL-resistant A2058 cells were also more resistant to the cytotoxicity of all these OXOPHOS inhibitors. As a result, antimycin A and FCCP at the maximal concentrations caused only a modest decrease in their viability (maximum of 30% decrease) (Fig. 5B). However, both antimycin A and FCCP enhanced

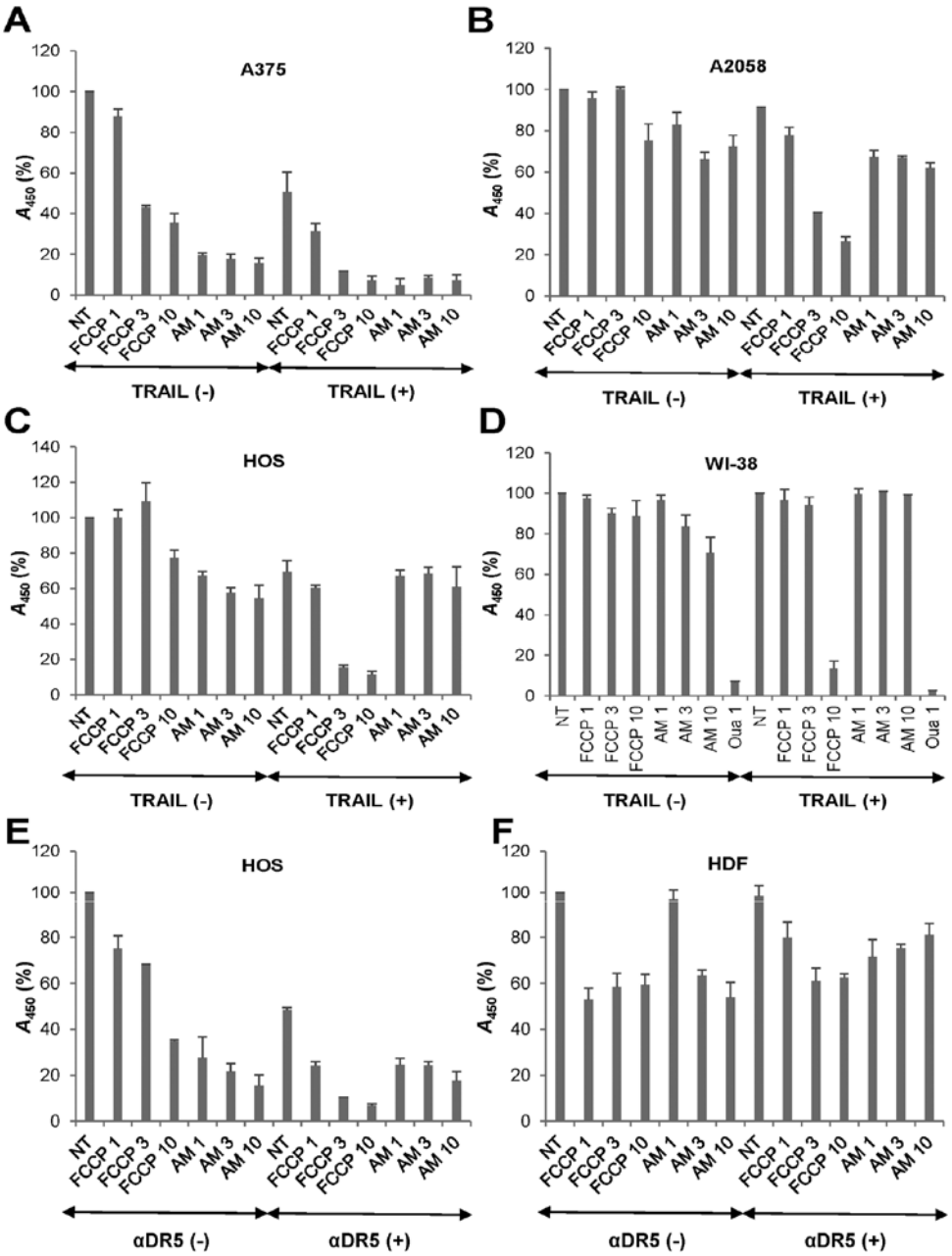

Figure 5. OXOPHOS inhibitors potentiate TRAIL cytotoxicity in a tumor-selective manner. A375 (A), A2058 (B), HOS (C and E), WI-38 (D), and HDF (F) were treated with 100 ng/ml TRAIL or 1 μg/ml agonistic anti-DR5 antibody (αDR5), 1, 3 and 10 μM FCCP and 1, 3 and 10 μg/ml antimycin A (AM) alone or in combination for 72 h. Then, the cells were measured for viability using WST-8 assay in triplicates. The data show means ± SD in a representative experiment (N=3).

TRAIL cytotoxicity at the nontoxic concentrations. OS cell lines including HOS cells were more resistant than MM cells to all these OXOPHOS inhibitors. FCCP also sensitized the cells while antimycin A had a slight sensitizing effect (Fig. 5C). To determine whether the effect of OXOPHOS inhibitors is selective for tumor cells, we analyzed the impact of TRAIL and OXOPHOS inhibitor alone or in combination on the growth of non-transformed cells. FCCP and antimycin A ≤10 μM had the minimal effects on the growth of WI-38 fibroblasts (Fig. 5D). Treatment with TRAIL + FCCP or TRAIL + antimycin A had a marginal effect on their growth (maximum of 14% reduction at 10 μM FCCP). The tolerance to TRAIL and OXOPHOS inhibitors alone or in combination was specific since 1 μM ouabain heavily killed the cells. Likewise TRAIL, the agonistic antibody against DR5 (αDR5) also synergistically killed HOS cells with FCCP and antimycin A (Fig. 5E). HDF was highly resistant to αDR5 and either OXOPHOS inhibitor alone or in combination (Fig. 5F). These results indicate that OXOPHOS inhibitors potentiate TRAIL cytotoxicity in a tumor-selective manner.

OXOPHOS inhibitors amplify both caspase-dependent and caspase-independent cell death in MM and OS cells at different time-points. To determine the cell death modality enhanced by OXOPHOS inhibitors, we examined the effect of FCCP on caspase-3/7 activation and 7-AAD staining simultaneously. FCCP amplified TRAIL-induced caspase-3/7 activation in A2058 cells during 24 h. Both

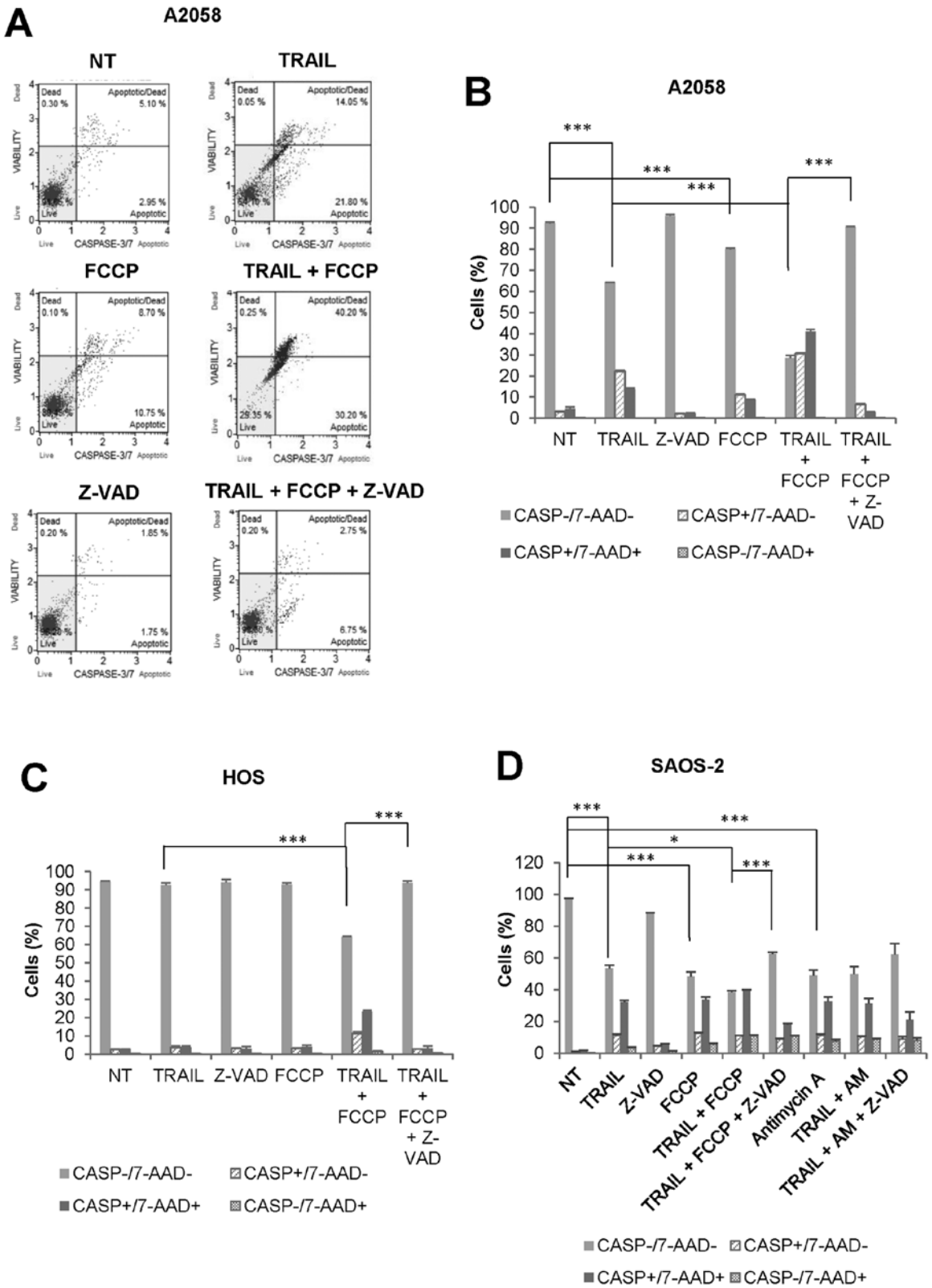

Figure 6. OXOPHOS inhibitors amplify both caspase-dependent and caspase-independent cell death in MM and OS cells at different time-points. A2058 (A and B), HOS (C), and SAOS-2 cells (D) were treated with 100 ng/ml TRAIL, 3 μM FCCP or 3 μg/ml antimycin A (AM) alone or in combination in the presence or absence of 10 μM z-VAD-FMK (Z-VAD) for 24 (A-C) or 72 h (D). Then the cells were analyzed in triplicates for caspase-3/7 activation and membrane integrity using NucView and 7-amino-actinomycin D (7-AAD) in a Muse Cell Analyzer. The data show means ± SD in a representative experiment (N=3). Data were analyzed by ANOVA followed by the Tukey's post hoc $^{*}P<0.05$; $^{***}P<0.001$.

caspase-3/7-activated, 7-AAD-negative ($CASP^{+}/7\text{-}AAD^{-}$) cells and caspase-3/7-activated, 7-AAD-positive ($CASP^{+}/7\text{-}AAD^{+}$) cells were increased, and Z-VAD-FMK entirely inhibited the effects (Fig. 6A and B). Meanwhile, caspase-3/7-inactivated, 7-AAD-positive ($CASP^{-}/7\text{-}AAD^{+}$) cells were minimally increased by TRAIL and FCCP alone or in combination. We

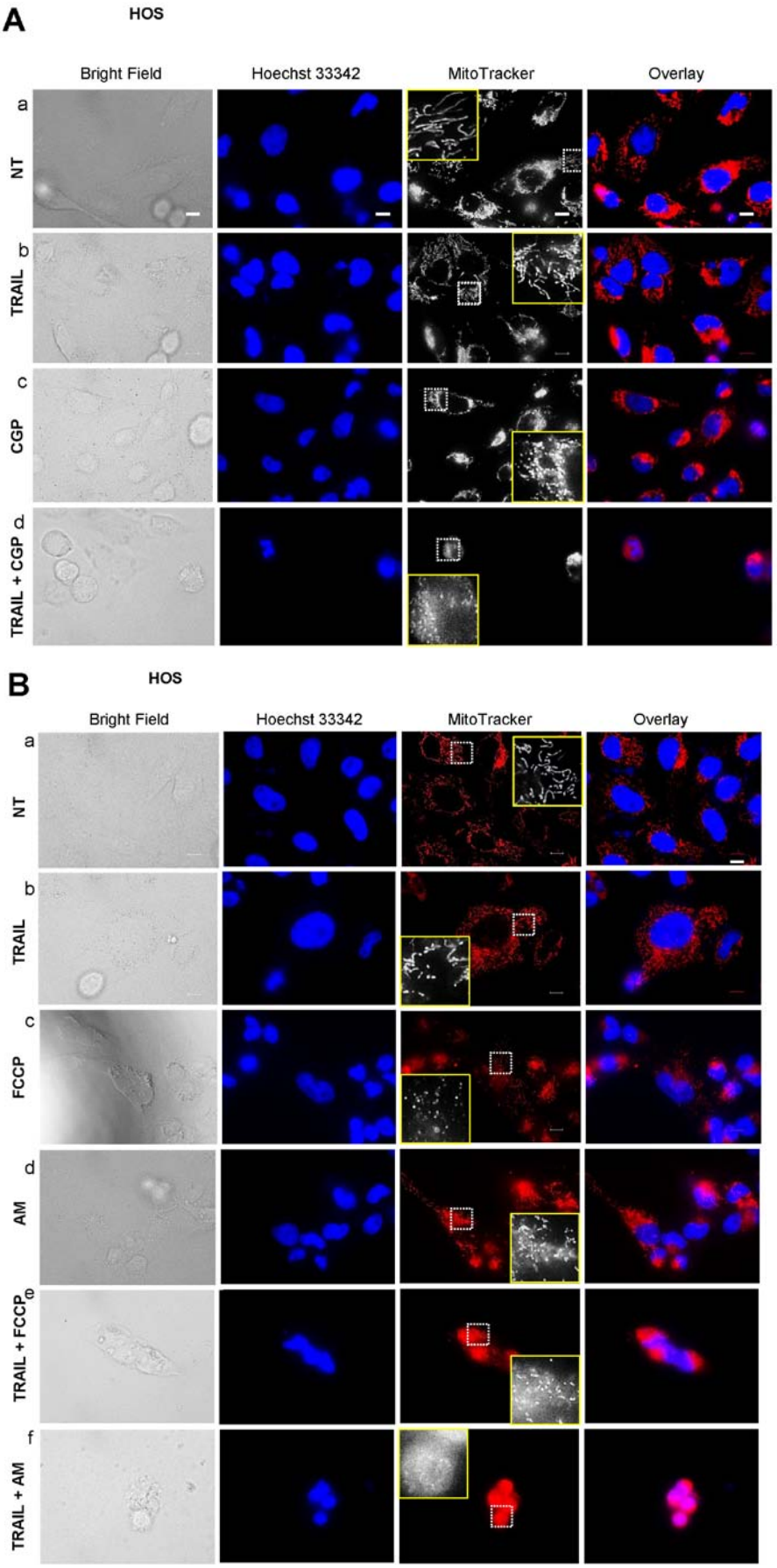

Figure 7. Mitochondrial Ca^{2+} overload induces mitochondrial fragmentation and potentiates TRAIL-induced mitochondrial network disruption. HOS cells were treated with 100 ng/ml TRAIL and 10 μM CGP-37157 (A), 3 μM FCCP or 3 μg/ml antimycin A (AM) (B) alone or in combination for 24 h at 37˚C. After washing, the cells were stained with Hoechst 33342 and MitoTracker Red CMXRos for 1 h and washed again. Images were obtained using a BZ X-700 Fluorescence Microscope equipped with a 100x, 1.40 n.a. UPlanSApo Super-Apochromat, coverslip-corrected oil objective and analyzed using BZ-H3A application software and free NIH ImageJ software. Bar, 10 μm.

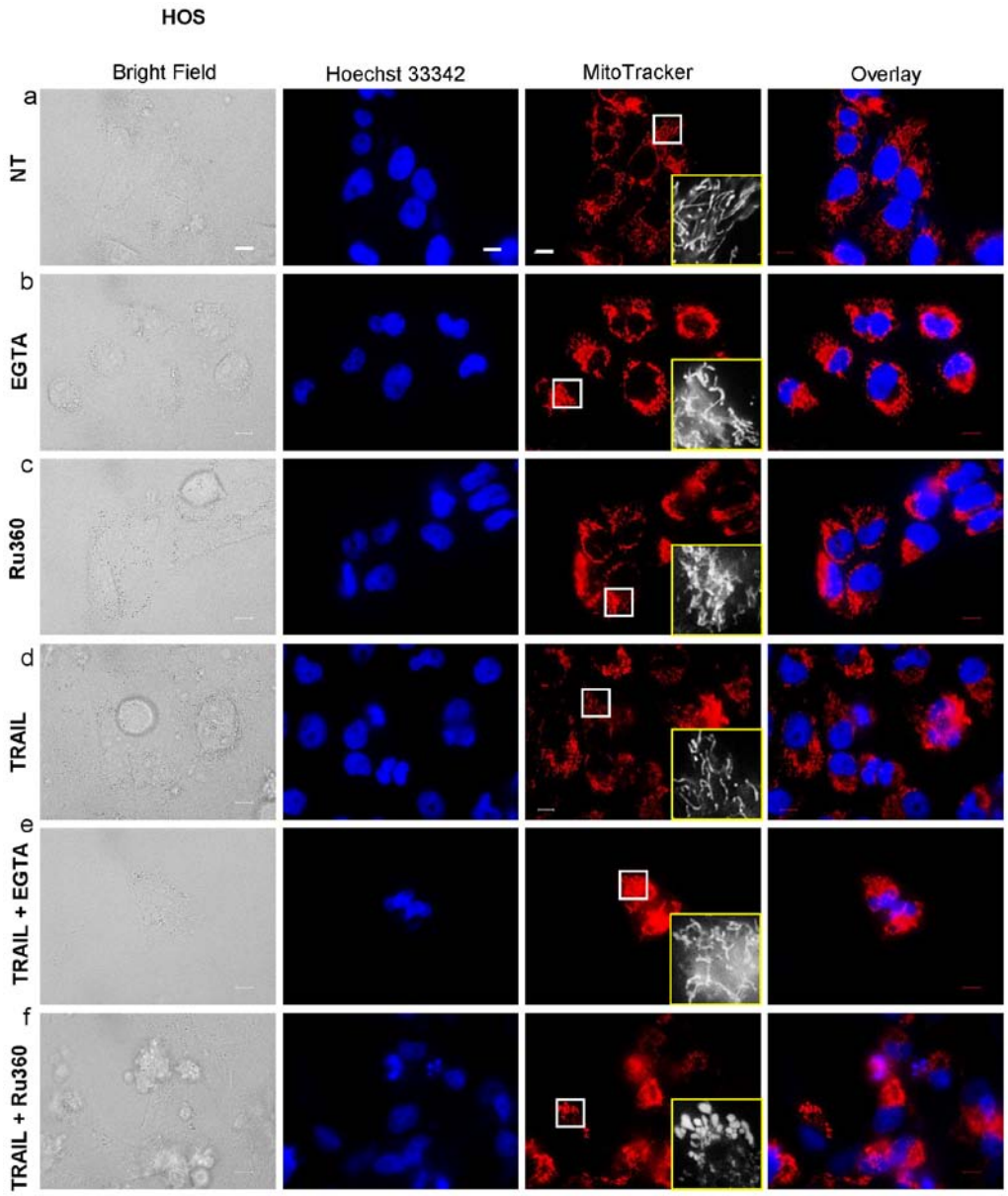

Figure 8. Mitochondrial Ca^{2+} removal causes mitochondrial hyperfusion and potentiates TRAIL-induced mitochondrial network disruption. HOS cells were treated with 100 ng/ml TRAIL and 0.5 mM EGTA or 1 μM Ruthenium 360 (Ru360) alone or in combination for 24 h at 37˚C. After washing, the cells were stained with Hoechst 33342 and MitoTracker Red CMXRos for 1 h, and washed again. Images were obtained and analyzed as described in the legend of Fig. 7. Bar, 10 μm.

obtained similar results with HOS cells (Fig. 6C). The cytotoxicity of TRAIL, as well as OXOPHOS inhibitors, became more pronounced under prolonged incubation conditions (72 h). Fig. 6D shows the representative results obtained with SAOS-2 cells. TRAIL, FCCP, and antimycin A reduced cell viability to a similar extent. Concomitantly, $CASP^+/7\text{-}AAD^+$ cells were increased to comparable levels. In addition, when TRAIL and FCCP applied in combination, $CASP^-/7\text{-}AAD^+$ cells were significantly increased compared with either agent alone (10.95±0.35 for TRAIL + FCCP, 3.4±0.6 for TRAIL, 5.6±0.7 for FCCP, $p<0.01$ vs TRAIL alone, $P<0.05$ vs FCCP alone, N=3). In contrast, the effect of the combined application of TRAIL and antimycin A was almost comparable to that of antimycin A alone. Moreover, the cell death by TRAIL + either OXOPHOS inhibitor was inhibited partially, but not completely by Z-VAD-FMK. Collectively, these results indicate that OXOPHOS inhibitors amplify both caspase-dependent and caspase-independent cell death at different time-points.

Mitochondrial Ca^{2+} overload induces mitochondrial fragmentation and potentiates TRAIL-induced mitochondrial network disruption. Previously, we reported that TRAIL modulates the mitochondrial network dynamics in a tumor-selective manner and that this effect is critical for TRAIL cytotoxicity (34). The facts led us to hypothesize that the potentiation of TRAIL cytotoxicity might be related to increased mitochondrial network abnormalities. To test this, we analyzed the effect of the Ca^{2+}-modulating agents on the mitochondrial network using HOS cells as a model. Most healthy HOS cells were highly adherent and possessed tubular mitochondria around healthy nuclei (Fig. 7A-a). Treatment with TRAIL for 24 h resulted in the minimal changes in their morphology and a

modest fragmentation of the mitochondria (Fig. 7A-b) while CGP treatment led to a substantial increase in round cells that possess punctate mitochondria and damaged nuclei (Fig. 7A-c). When TRAIL and CGP-37157 were used in combination, the mitochondria became more fragmented and clustered, and the nuclei had smaller fragments (Fig. 7A-d). Also, the red signals were overlapped with the blue signals, thereby resulting in the appearance in the pink signals. FCCP and antimycin A also led to a massive increase in round cells and punctate mitochondria while the nuclei were damaged only modestly (Fig. 7B-c and -d). Meanwhile, when TRAIL and either agent were used together, most cells became heavily damaged and detached from the coverslips. Accordingly, only a small population of the damaged cells remained on the coverslips. The remained cells possessed punctate, clustered mitochondria and fragmented nuclei. Also, the overlapping of the red and the blue signals became more pronounced (Fig. 7B-e and -f). These results indicate that mitochondrial Ca^{2+} overload induces mitochondrial fragmentation and potentiates TRAIL-induced mitochondrial network disruption.

Mitochondrial Ca^{2+} removal causes mitochondrial hyperfusion and potentiates TRAIL-induced mitochondrial network disruption. The data presented above suggested that mitochondrial Ca^{2+} overload promoted mitochondrial fragmentation, suggesting that the Ca^{2+} regulates mitochondrial fission positively. To further elucidate the functional link between mitochondrial Ca^{2+} and the mitochondrial dynamics, we examined the effects of EGTA and Ru360 on the mitochondrial network. Either EGTA or Ru360 alone led to a robust mitochondrial hyperfusion, as indicated by the appearance in elongated, highly interconnected mitochondria (Fig. 8-b and -c). Either agent alone had the minimal effects on the cellular and nuclear morphology. However, TRAIL + Ru360, but not TRAIL + EGTA, severely damaged the cells and the mitochondria became punctate and clustered, and the nuclei became fragmented (Fig. 8-f). Concomitantly, most red signals became overlapped with the blue signals, thereby generating pink signals, as observed in the case of the application of TRAIL + CGP or TRAIL + OXOPHOS inhibitors. These results show that mitochondrial Ca^{2+} removal induces mitochondrial hyperfusion and eventually potentiates TRAIL-induced mitochondrial network disruption.

Discussion

The present study demonstrated that TRAIL-resistant MM and OS cells were tolerant to mitochondrial Ca^{2+} overload by the drug (Fig. 1). Strikingly, the basal $[Ca^{2+}]_{mit}$ spontaneously declined over time in these cells, indicating the activation of a certain mechanism for Ca^{2+} efflux from the mitochondrial matrix. NCLX (35-37) and MPTPs (41,42) participate in mitochondrial Ca^{2+} extrusion in normal cells and some tumor cells. Therefore, it was possible that either or both pathways contribute to the tolerance. Consistent with this view, the present study demonstrates that NCLX plays a key role in mitochondrial Ca^{2+} extrusion, thereby specifically regulating $[Ca^{2+}]_{mit}$ in MM and OS cells (Fig. 2C and D). Accordingly, CGP-37157 treatment led to a persistent mitochondrial Ca^{2+} rise in all MM and OS cell lines tested. It is well-known that mitochondrial Ca^{2+} has a dual function depending on its magnitude and duration. Ca^{2+} accumulated in the mitochondrial matrix plays a critical role in aerobic metabolism and cell survival while a persistent Ca^{2+} overload is the primary cause of apoptosis (17,19). The present study demonstrated that CGP-37157 sensitized MM and OS cells to TRAIL cytotoxicity. Z-VAD-FMK strongly blocked the effect, and CGP-37157 significantly increased caspase-3/7 activation (Fig. 3). The results suggest that the persistent Ca^{2+} overload primarily promotes apoptosis. Our results are similar to those reported by another group in prostate cancer cells (43,44). The previous reports showed that CGP-37157 led to mitochondrial Ca^{2+} overload and sensitized the cells to TRAIL-induced apoptosis. Thus, NCLX seems to play a critical role in the regulation of mitochondrial Ca^{2+} dynamics and TRAIL sensitivity in cancer types from different origins. Moreover, we found that OXOPHOS inhibitors such as FCCP and antimycin A also caused mitochondrial Ca^{2+} overload (Fig. 4) and amplified TRAIL cytotoxicity toward MM and OS cells (Fig. 5). These two agents strongly sensitized all MM and OS cell lines including those relatively tolerant to the effect of CGP-37157. As expected, likewise CGP-37157, the OXOPHOS inhibitors significantly enhanced TRAIL-induced caspase-3/7 activation, and Z-VAD-FMK strongly blocked the effects (Fig. 6), supporting the view that apoptosis is the primary target in the Ca^{2+}-dependent TRAIL sensitization. Nevertheless, our data suggested that mitochondrial Ca^{2+} overload could also promote another caspase-independent cell death. It is noteworthy that distinct cell death modalities seemed to be encouraged by CGP-37157 and OXOPHOS inhibitors at different time-points. At the early time (within 24 h of post-treatment), apoptosis was mainly enhanced, as indicated by increased caspase-3/7 activation and the complete blockade by the caspase inhibitor (Figs. 3 and 6). Whereas, at the late time (72 h), the additional nonapoptotic cell death was primarily amplified. Interestingly, at that point OXOPHOS inhibitors alone caused a substantial cell killing comparable to that induced by TRAIL, and the simultaneous application of TRAIL had the minimal additional cytotoxic effect. At present, the reason for such switching in the cell death modality remains unclear. However, energy deprivation under the prolonged cell cultivation might somewhat participate in this switching. In support of this view, we noticed that similar switching of cell death modalities from apoptosis to non-apoptotic death occurred upon mitochondrial Ca^{2+} removal (24). Alternatively, autophagy caused by energy depletion might modulate the cell death modality. Of note, TRAIL induces autophagy in various cancer cell types, including MM cells, and autophagy prevents apoptosis in these cells (45,46). Alternatively, TRAIL might induce necroptosis, a non-apoptotic programmed cell death, in the late stage since recent studies revealed that TRAIL could induce both apoptosis and necroptosis depending on the cellular caspase-8 activation and autophagy status (9,47,48). Mitochondrial Ca^{2+} overload has also been shown to cause necrosis (17). In fact, we observed a significant increase in the cell population with necrotic cell death ($CASP^-$/7-AAD^+) upon stimulation with TRAIL + the OXOPHOS inhibitors. However, the cell population was still small (~11%), and our preliminary experiments showed that necrostatin-1, a specific necroptosis inhibitor, reduced the slow cell death only modestly. These results suggest that necroptosis/necrosis plays a minor role in

the slow cell death, but further investigation is necessary to clarify the role.

Another important finding in the present study is that the Ca^{2+}-dependent TRAIL sensitization functionally links to the mitochondrial fission-fusion dynamics. Our results demonstrated that all the Ca^{2+}-modulating agents markedly altered the mitochondrial dynamics. Specifically, agents inducing mitochondrial Ca^{2+} overloads such as CGP-37157 and the OXOPHOS inhibitors led to mitochondrial fragmentation (Fig. 7) while that causing mitochondrial Ca^{2+} depletion such as EGTA and Ru360 evoked mitochondrial hyperfusion (Fig. 8). Moreover, regardless of their reciprocal actions on the mitochondrial dynamics, the two types of agents commonly exacerbated mitochondrial network collapse by TRAIL (Figs. 7 and 8). These findings strongly suggest that an appropriate level of mitochondrial Ca^{2+} is essential for maintaining the mitochondrial dynamics homeostasis. Our results might provide insight into the controversial observations on the role of mitochondrial fission in apoptosis. Some studies demonstrate the requirement of mitochondrial fission machinery including Drp1, Fis1, and Opa1 in pro-apoptotic events such as cytochrome *c* release and apoptosis (28-30). Whereas, other studies demonstrated that mitochondrial fission is pro-survival and its inhibition promoted apoptosis (31-33). It is noteworthy that at least in cancer cells such as prostate (44) mitochondrial fragmentation by itself is insufficient for inducing apoptosis. Our previous study demonstrated that both an excess fragmentation of the mitochondria and the subsequent clustering of the fragmented mitochondria were essential for TRAIL-induced apoptosis in MM and OS cells (34). The fragmentation and clustering of the mitochondria occurred in a tumor-selective manner and distinct from the usual Drp1-dependent mitochondrial fission process because they were accelerated rather than reduced by inhibition or knockdown of Drp1 (33). This observation strongly suggests that Drp1-dependent reversible mitochondrial fission may prevent the pro-apoptotic mitochondrial network abnormalities, thereby serving as a pro-survival event. On the other hand, an excess irreversible Drp1-independent mitochondrial fragmentation in conjunction with abnormal clustering may be irreversibly committed to mitochondrial dysfunction, thereby serving a pro-apoptotic event. Consistent with this view, another group has reported that mitochondrial aggregation preceded cytochrome *c* release and apoptosis in arsenic trioxide-treated human glioblastoma cells (49,50). Collectively, it is likely that an appropriate level of mitochondrial Ca^{2+} is required for the pro-survival reversible mitochondrial fission, thereby preventing the pro-death mitochondrial network collapse. Further studies to prove this scenario are underway in our laboratory.

In conclusion, we demonstrate in this report that mitochondrial Ca^{2+} plays a vital role in maintaining the mitochondrial dynamics and cell survival in MM and OS cells. Thus, targeting mitochondrial Ca^{2+} homeostasis may serve as a promising approach to overcome the TRAIL resistance of these cancers without compromising the tumor-selectivity.

Acknowledgements

The authors thank Dr T. Ando for kindly providing TE85 and 143B cells. We also appreciate Drs T. Tokunaga, T. Ito, and A. Onoe for their technical assistance. This study was supported in part by JSPS KAKENHI grant no. 15K09750 to Y.S.K.

References

1. Almasan A and Ashkenazi A: Apo2L/TRAIL: Apoptosis signaling, biology, and potential for cancer therapy. Cytokine Growth Factor Rev 14: 337-348, 2003.
2. Johnstone RW, Frew AJ and Smyth MJ: The TRAIL apoptotic pathway in cancer onset, progression and therapy. Nat Rev Cancer 8: 782-798, 2008.
3. Wang S: The promise of cancer therapeutics targeting the TNF-related apoptosis-inducing ligand and TRAIL receptor pathway. Oncogene 27: 6207-6215, 2008.
4. Gonzalvez F and Ashkenazi A: New insights into apoptosis signaling by Apo2L/TRAIL. Oncogene 29: 4752-4765, 2010.
5. Kischkel FC, Lawrence DA, Chuntharapai A, Schow P, Kim KJ and Ashkenazi A: Apo2L/TRAIL-dependent recruitment of endogenous FADD and caspase-8 to death receptors 4 and 5. Immunity 12: 611-620, 2000.
6. LeBlanc HN and Ashkenazi A: Apo2L/TRAIL and its death and decoy receptors. Cell Death Differ 10: 66-75, 2003.
7. Herrero-Martín G, Høyer-Hansen M, García-García C, Fumarola C, Farkas T, López-Rivas A and Jäättelä M: TAK1 activates AMPK-dependent cytoprotective autophagy in TRAIL-treated epithelial cells. EMBO J 28: 677-685, 2009.
8. He W, Wang Q, Xu J, Xu X, Padilla MT, Ren G, Gou X and Lin Y: Attenuation of TNFSF10/TRAIL-induced apoptosis by an autophagic survival pathway involving TRAF2- and RIPK1/RIP1-mediated MAPK8/JNK activation. Autophagy 8: 1811-1821, 2012.
9. Jouan-Lanhouet S, Arshad MI, Piquet-Pellorce C, Martin-Chouly C, Le Moigne-Muller G, Van Herreweghe F, Takahashi N, Sergent O, Lagadic-Gossmann D, Vandenabeele P, *et al*: TRAIL induces necroptosis involving RIPK1/RIPK3-dependent PARP-1 activation. Cell Death Differ 19: 2003-2014, 2012.
10. Sosna J, Philipp S, Fuchslocher Chico J, Saggau C, Fritsch J, Föll A, Plenge J, Arenz C, Pinkert T, Kalthoff H, *et al*: Differences and similarities in TRAIL- and tumor necrosis factor-mediated necroptotic signaling in cancer cells. Mol Cell Biol 36: 2626-2644, 2016.
11. Ivanov VN, Bhoumik A and Ronai Z: Death receptors and melanoma resistance to apoptosis. Oncogene 22: 3152-3161, 2003.
12. Dyer MJ, MacFarlane M and Cohen GM: Barriers to effective TRAIL-targeted therapy of malignancy. J Clin Oncol 25: 25: 4505-4506, 2007.
13. Dimberg LY, Anderson CK, Camidge R, Behbakht K, Thorburn A and Ford HL: On the TRAIL to successful cancer therapy? Predicting and counteracting resistance against TRAIL-based therapeutics. Oncogene 32: 1341-1350, 2013.
14. Guiho R, Biteau K, Heymann D and Redini F: TRAIL-based therapy in pediatric bone tumors: How to overcome resistance. Future Oncol 11: 535-542, 2015.
15. de Miguel D, Lemke J, Anel A, Walczak H and Martinez-Lostao L: Onto better TRAILs for cancer treatment. Cell Death Differ 23: 733-747, 2016.
16. Elustondo PA, Nichols M, Robertson GS and Pavlov EV: Mitochondrial Ca(2+) uptake pathways. J Bioenerg Biomembr 49: 113-119, 2017.
17. Bonora M, Wieckowski MR, Chinopoulos C, Kepp O, Kroemer G, Galluzzi L and Pinton P: Molecular mechanisms of cell death: Central implication of ATP synthase in mitochondrial permeability transition. Oncogene 34: 1475-1486, 2015.
18. Izzo V, Bravo-San Pedro JM, Sica V, Kroemer G and Galluzzi L: Mitochondrial permeability transition: New findings and persisting uncertainties. Trends Cell Biol 26: 655-667, 2016.
19. Galluzzi L, Bravo-San Pedro JM, Kepp O and Kroemer G: Regulated cell death and adaptive stress responses. Cell Mol Life Sci 73: 2405-2410, 2016.
20. Orrenius S, Gogvadze V and Zhivotovsky B: Calcium and mitochondria in the regulation of cell death. Biochem Biophys Res Commun 460: 72-81, 2015.
21. Danese A, Patergnani S, Bonora M, Wieckowski MR, Previati M, Giorgi C and Pinton P: Calcium regulates cell death in cancer: Roles of the mitochondria and mitochondria-associated membranes (MAMs). Biochim Biophys Acta 1858: 615-627, 2017.

22. Marchi S and Pinton P: Alterations of calcium homeostasis in cancer cells. Curr Opin Pharmacol 29: 1-6, 2016.
23. Monteith GR, Prevarskaya N and Roberts-Thomson SJ: The calcium-cancer signalling nexus. Nat Rev Cancer 17: 367-380, 2017.
24. Takata N, Ohshima Y, Suzuki-Karasaki M, Yoshida Y, Tokuhashi Y and Suzuki-Karasaki Y: Mitochondrial Ca^{2+} removal amplifies TRAIL cytotoxicity toward apoptosis-resistant tumor cells via promotion of multiple cell death modalities. Int J Oncol 51: 193-203, 2017.
25. Elgass K, Pakay J, Ryan MT and Palmer CS: Recent advances into the understanding of mitochondrial fission. Biochim Biophys Acta 1833: 150-161, 2013.
26. Chang CR and Blackstone C: Dynamic regulation of mitochondrial fission through modification of the dynamin-related protein Drp1. Ann NY Acad Sci 1201: 34-39, 2010.
27. Senft D and Ronai ZA: Regulators of mitochondrial dynamics in cancer. Curr Opin Cell Biol 39: 43-52, 2016.
28. Frank S, Gaume B, Bergmann-Leitner ES, Leitner WW, Robert EG, Catez F, Smith CL and Youle RJ: The role of dynamin-related protein 1, a mediator of mitochondrial fission, in apoptosis. Dev Cell 1: 515-525, 2001.
29. Lee YJ, Jeong SY, Karbowski M, Smith CL and Youle RJ: Roles of the mammalian mitochondrial fission and fusion mediators Fis1, Drp1, and Opa1 in apoptosis. Mol Biol Cell 15: 5001-5011, 2004.
30. Estaquier J and Arnoult D: Inhibiting Drp1-mediated mitochondrial fission selectively prevents the release of cytochrome *c* during apoptosis. Cell Death Differ 14: 1086-1094, 2007.
31. Rehman J, Zhang HJ, Toth PT, Zhang Y, Marsboom G, Hong Z, Salgia R, Husain AN, Wietholt C and Archer SL: Inhibition of mitochondrial fission prevents cell cycle progression in lung cancer. FASEB J 26: 2175-2186, 2012.
32. Westrate LM, Sayfie AD, Burgenske DM and MacKeigan JP: Persistent mitochondrial hyperfusion promotes G2/M accumulation and caspase-dependent cell death. PLoS One 9: e91911, 2014.
33. Akita M, Suzuki-Karasaki M, Fujiwara K, Nakagawa C, Soma M, Yoshida Y, Ochiai T, Tokuhashi Y and Suzuki-Karasaki Y: Mitochondrial division inhibitor-1 induces mitochondrial hyperfusion and sensitizes human cancer cells to TRAIL-induced apoptosis. Int J Oncol 45: 1901-1912, 2014.
34. Suzuki-Karasaki Y, Fujiwara K, Saito K, Suzuki-Karasaki M, Ochiai T and Soma M: Distinct effects of TRAIL on the mitochondrial network in human cancer cells and normal cells: Role of plasma membrane depolarization. Oncotarget 6: 21572-21588, 2015.
35. Nita II, Hershfinkel M, Kantor C, Rutter GA, Lewis EC and Sekler I: Pancreatic β-cell Na^+ channels control global Ca^{2+} signaling and oxidative metabolism by inducing Na^+ and Ca^{2+} responses that are propagated into mitochondria. FASEB J 28: 3301-3312, 2014.
36. Ruiz A, Alberdi E and Matute C: CGP37157, an inhibitor of the mitochondrial Na+/Ca^{2+} exchanger, protects neurons from excitotoxicity by blocking voltage-gated Ca^{2+} channels. Cell Death Dis 5: e1156, 2014.
37. Ben-Hail D, Palty R and Shoshan-Barmatz V: Measurement of mitochondrial Ca^{2+} transport mediated by three transport proteins: VDAC1, the Na^+/Ca^{2+} exchanger, and the Ca^{2+} uniporter. Cold Spring Harb Protoc 2014: 161-166, 2014.
38. Izeradjene K, Douglas L, Tillman DM, Delaney AB and Houghton JA: Reactive oxygen species regulate caspase activation in tumor necrosis factor-related apoptosis-inducing ligand-resistant human colon carcinoma cell lines. Cancer Res 65: 7436-7445, 2005.
39. Inoue T and Suzuki-Karasaki Y: Mitochondrial superoxide mediates mitochondrial and endoplasmic reticulum dysfunctions in TRAIL-induced apoptosis in Jurkat cells. Free Radic Biol Med 61: 273-284, 2013.
40. Suzuki-Karasaki M, Ochiai T and Suzuki-Karasaki Y: Crosstalk between mitochondrial ROS and depolarization in the potentiation of TRAIL-induced apoptosis in human tumor cells. Int J Oncol 44: 616-628, 2014.
41. Bernardi P and von Stockum S: The permeability transition pore as a Ca(2+) release channel: New answers to an old question. Cell Calcium 52: 22-27, 2012.
42. Gutiérrez-Aguilar M and Baines CP: Structural mechanisms of cyclophilin D-dependent control of the mitochondrial permeability transition pore. Biochim Biophys Acta 1850: 2041-2047, 2015.
43. Kaddour-Djebbar I, Lakshmikanthan V, Shirley RB, Ma Y, Lewis RW and Kumar MV: Therapeutic advantage of combining calcium channel blockers and TRAIL in prostate cancer. Mol Cancer Ther 5: 1958-1966, 2006.
44. Kaddour-Djebbar I, Choudhary V, Brooks C, Ghazaly T, Lakshmikanthan V, Dong Z and Kumar MV: Specific mitochondrial calcium overload induces mitochondrial fission in prostate cancer cells. Int J Oncol 36: 1437-1444, 2010.
45. Han J, Hou W, Goldstein LA, Lu C, Stolz DB, Yin XM and Rabinowich H: Involvement of protective autophagy in TRAIL resistance of apoptosis-defective tumor cells. J Biol Chem 283: 19665-19677, 2008.
46. Hou W, Han J, Lu C, Goldstein LA and Rabinowich H: Enhancement of tumor-TRAIL susceptibility by modulation of autophagy. Autophagy 4: 940-943, 2008.
47. Nikoletopoulou V, Markaki M, Palikaras K and Tavernarakis N: Crosstalk between apoptosis, necrosis and autophagy. Biochim Biophys Acta 1833: 3448-3459, 2013.
48. Goodall ML, Fitzwalter BE, Zahedi S, Wu M, Rodriguez D, Mulcahy-Levy JM, Green DR, Morgan M, Cramer SD and Thorburn A: The autophagy machinery controls cell death switching between apoptosis and necroptosis. Dev Cell 37: 337-349, 2016.
49. Haga N, Fujita N and Tsuruo T: Mitochondrial aggregation precedes cytochrome *c* release from mitochondria during apoptosis. Oncogene 22: 5579-5585, 2003.
50. Haga N, Fujita N and Tsuruo T: Involvement of mitochondrial aggregation in arsenic trioxide (As_2O_3)-induced apoptosis in human glioblastoma cells. Cancer Sci 96: 825-833, 2005.